

Effect of *Crotalus viridis viridis* snake venom on the ultrastructure and intracellular survival of *Trypanosoma cruzi*

CAMILA M. ADADE¹, BRUNO LEMOS CONS², PAULO A. MELO² and THAÏS SOUTO-PADRÓN^{1*}

¹ *Laboratório de Biologia Celular e Ultraestrutura, Departamento de Microbiologia Geral, Instituto de Microbiologia Prof. Paulo de Góes, Centro de Ciências da Saúde, bloco I, Universidade Federal do Rio de Janeiro, Ilha do Fundão, Rio de Janeiro, Brazil*

² *Laboratório de Farmacologia das Toxinas e Substâncias Antagonistas, Centro de Ciências da Saúde, bloco J, Universidade Federal do Rio de Janeiro, Ilha do Fundão, Rio de Janeiro, Brazil*

(Received 22 March 2010; revised 19 May 2010; accepted 31 May 2010; first published online 21 July 2010)

SUMMARY

Chagas' disease, caused by *Trypanosoma cruzi*, affects 16–18 million people in Central and South America. Patient treatment is based on drugs that have toxic effects and limited efficacy. Therefore, new chemotherapeutic agents need to be developed. Snake venoms are sources of natural compounds used in various medical treatments. We observed that *Crotalus viridis viridis* venom was effective against all developmental forms of *T. cruzi*. Ultrastructural analysis revealed swelling of mitochondria, blebbing and disruption of the plasma membrane, loss of cytoplasm components and morphological changes of the cell. Staining with propidium iodide and rhodamine 123 confirmed the observed alterations in the plasma and mitochondrial membranes, respectively. The effects of the venom on the parasite intracellular cycle were also analysed. Pre-infected LLC-MK₂ cells incubated with *Cvv* venom showed a 76–93% reduction in the number of parasites per infected cell and a 94–97.4% reduction in the number of parasites per 100 cells after 96 h of infection. Free trypomastigotes harvested from the supernatants of *Cvv* venom-treated cells were incapable of initiating a new infection cycle. Our data demonstrate that *Cvv* venom can access the host cell cytoplasm at concentrations that cause toxicity only to the amastigote forms of *T. cruzi*, and yields altered parasites with limited infective capacity, suggesting the potential use of *Cvv* venom in Chagas' disease chemotherapy.

Key words: *Crotalus viridis viridis*, *Trypanosoma cruzi*, Chagas' disease chemotherapy, ultrastructure, snake venom.

INTRODUCTION

Trypanosoma cruzi is the aetiological agent of Chagas' disease, which remains a major public health issue in Latin America where approximately 100 million people are at risk. Human hosts are naturally infected by the bite of the insect vector (Hemiptera: Reduviidae), but blood transfusion, congenital transmission and ingestion of contaminated food are also important mechanisms of infection (Moncayo and Silveira, 2009). The chronic phase of the disease mostly occurs several years after infection, and it is characterized by severe cardiac and gastrointestinal pathologies (Coura and De Castro, 2002). Treatment of chagasic patients relies on 2 nitroheterocyclic drugs that have several limitations due to their high toxicity and have minimal benefits during the chronic phase of the disease (Urbina and Docampo, 2003). These restrictions encourage the search for alternative synthetic or natural compounds that are effective

for both clinical treatment of Chagas disease and chemoprophylaxis in donated blood.

Animal venoms have been used in the treatment of a variety of pathophysiological conditions in Ayurveda, homeopathy and folk medicine. With the advent of biotechnology, the efficacy of such treatments has improved with the purification of venom components and the delineation of their therapeutic properties. Snake venoms are complex mixtures of proteins, nucleotides and inorganic ions (Koh *et al.* 2006) with a high degree of target specificity. They have been increasingly used as pharmacological tools and prototypes for drug development, including in cancer chemotherapy (Newman *et al.* 1993; Pai *et al.* 1996; Zhou *et al.* 2000; Corrêa Jr. *et al.* 2002; Papo and Shai, 2003; Papo *et al.* 2003, 2004; Araya and Lomonte, 2007; El-Rafael and Sarkar, 2009). One of these drugs, Captopril, is the first commercial inhibitor of angiotensin I-converting enzyme (ACE) and is used for the treatment of human hypertension. This compound was developed from studies of *Bothrops jararaca* venom and its bradykinin-potentiating peptides (BPPs) (Fernandez *et al.* 2004).

Snake venom proteins have been used to kill HIV (Zhang *et al.* 2003), the protozoan parasites *Plasmodium falciparum* (Zieler *et al.* 2001) and

* Corresponding author: Laboratório de Biologia Celular e Ultraestrutura, Instituto de Microbiologia Prof. Paulo de Góes, CCS, Bloco I, UFRJ, Ilha do Fundão, Rio de Janeiro, RJ, Brazil. Tel: +55 21 2562 6738. Fax: +5521 2560 8344. E-mail: souto.padron@micro.ufrj.br

Leishmania spp. (Fernandez-Gomez *et al.* 1994; Toyama *et al.* 2006; Tempone *et al.* 2007; Passero *et al.* 2007). Recent studies have revealed that the crude venom of South American *Bothrops* snakes inhibit the growth of *Leishmania major* promastigotes and *T. cruzi* epimastigotes (Gonçalves *et al.* 2002) and induce programmed cell death in *T. cruzi* (Deolindo *et al.* 2005). The L-amino acid oxidases are associated with the anti-protozoal activities observed in snake venoms of the *Bothrops* genera (Tempone *et al.* 2001; Ciscotto *et al.* 2009).

Other important snakes are those from the genus *Crotalus*, also known as rattlesnakes. Different species are present in the American continents, and *Crotalus durissus* and *C. viridis* are prevalent in South and North America, respectively (Tsai *et al.* 2003). The pathophysiological effects of *Crotalus* venoms are due to different enzymes and peptides that cause serious local effects such as oedema, haemorrhage and myonecrosis (Ownby *et al.* 1997).

Considering previous data obtained for other snake venoms against protozoa and the absence of a complete study investigating the activity of snake venoms during the entire *T. cruzi* cycle, we analysed the effect of *Crotalus viridis viridis* venom (Cvv venom) on the ultrastructure of all 3 developmental forms of this parasite and its effects on parasite intracellular development to investigate a possible target for its activity.

MATERIALS AND METHODS

Parasites

T. cruzi epimastigotes of the CL-Brener clone were maintained at 28 °C by weekly transfers in liver infusion tryptose (LIT) (Camargo, 1964) medium supplemented with 10% fetal calf serum (FCS). Four-day-old culture forms at the mid-log phase of growth were used in all experiments. Tissue culture trypomastigotes were obtained from the supernatants of 5 to 6-day-old infected LLC-MK₂ cells maintained in RPMI-1640 medium supplemented with 2% FCS at 37 °C in a 5% humidified CO₂ atmosphere as previously described (Bisaggio *et al.* 2006).

Parasite treatment

The Cvv crude venom was purchased from Sigma Chemical Co (St Louis, MO, USA). A stock solution was prepared at 50 mg/ml in phosphate-buffered saline (PBS, pH 7.2) and stored at -20 °C until use. Epimastigotes were resuspended in LIT medium at 5 × 10⁶ cells/ml, and a 1 ml aliquot of the suspension was added to the same volume of Cvv venom, which was previously diluted in LIT medium at twice the desired final concentration (0.25–500 µg/ml), in 24-well plates (Nunc Inc., Naperville, IL, USA). The samples were then incubated for 120 h at 28 °C.

The number of parasites was determined daily by counting formalin-fixed parasites using a Neubauer chamber. The LD₅₀, which corresponds to the drug concentration that inhibits 50% of cell growth, was used to estimate inhibition of proliferation. Parasites grown in venom-free LIT medium were used as a control. The growth experiments were carried out in triplicate, and the standard deviations of the cell densities at each time-point are indicated by the error bars. Parasite viability was monitored based on motility and trypan blue exclusion using light microscopy. Parasite suspensions (10 µl) were diluted in trypan blue solution (0.4% in water) at a 1:1 volume ratio and monitored by direct counting of viable and non-viable parasites using a Neubauer chamber.

Tissue-culture trypomastigotes were resuspended to a concentration of 1 × 10⁷ cells/ml in RPMI medium (Sigma) containing 10% FCS. This suspension (100 µl) was added to the same volume of the venom that had been previously diluted in RPMI medium at twice the desired final concentration (the same procedure used for epimastigotes treatment) in 96-well plates (Nunc Inc.), following incubation at 37 °C for 24 h. The LD₅₀ (50% trypomastigote lysis) was then calculated by cell counting of formalin-fixed parasites using a Neubauer chamber. The experiments were performed in triplicate, and at least 3 independent experiments were conducted.

The determination of the LD₅₀ for intracellular amastigotes is described below in the *Mammalian cell invasion by tissue-culture trypomastigotes* section.

Effect of boiled Cvv venom on parasite growth

Cvv venom was boiled for 7.5, 15 and 30 min at 95 °C (as previously described by Fernandez-Gomez *et al.* 1994) and was used to challenge epimastigote forms (CL-Brener clone). Epimastigotes were resuspended in LIT medium at 5 × 10⁶ cells/ml, incubated with 0.5 µg/ml (corresponding to the LD₅₀ previously obtained) of crude boiled and non-boiled (positive control) Cvv venom, and then incubated for 24, 48 and 72 h at 28 °C. The negative control consisted of parasites maintained in the same culture conditions but not exposed to venom. The number of parasites was determined daily by counting formalin-fixed parasites in a haemocytometer chamber as described previously.

Cvv venom cytotoxicity assay in non-infected LLC-MK₂ cells

Non-infected LLC-MK₂ cells were first submitted to Cvv venom treatment to determine the toxicity of the venom to host cells. Cells were seeded in 24-well plates containing glass cover-slips, cultivated in RPMI supplemented with 10% FCS, and then maintained at 37 °C in a 5% CO₂ humidified atmosphere

for 1 day as previously described (Bisaggio *et al.* 2008). After this period, the cultures were washed with PBS to remove non-adherent cells, cultivated in fresh RPMI medium containing 2% FCS and treated with 0.1, 10, 100 or 1000 $\mu\text{g}/\text{ml}$ of Cvv venom for up to 120 h. Control cells were subjected to the same procedure excluding the exposure to Cvv venom. The culture media were changed every 48 h. Cover-slips were collected daily, rinsed in PBS, fixed in Bouin's solution, stained with Giemsa and mounted onto glass slides with Permount (Fisher Scientific, NJ, USA). The number of adhered cells and the morphological characteristics of the cells were analysed.

The same procedure was performed in parallel to allow for analysis by the trypan blue exclusion test. Cover-slips were stained with a 1:1 volume dilution of trypan blue solution:RPMI medium and were observed using a Zeiss Axiovert light microscope (Oberkochen, Germany).

Mammalian cell invasion by tissue-culture trypomastigotes

To investigate the effect of Cvv venom on the intracellular cycle of the parasite, LLC-MK₂ cells were seeded in 24-well plates as described above. Thereafter, the cultures were washed and infected with tissue culture trypomastigotes (parasite:host cell ratio of 10:1). After 24 h of interaction, non-internalized parasites were removed by repeated washing with PBS, and the cells were cultivated in fresh RPMI medium containing 2% FCS with (37.5–500 ng/ml) or without snake venom (control cells). The media were changed every 2 days. Cover-slips were collected daily up to 96 h, rinsed in PBS, fixed in Bouin's solution, stained with Giemsa and mounted onto glass slides with Permount (Fisher Scientific, NJ, USA). Parasite infection was quantified using a Zeiss Axioplan 2 light microscope (Oberkochen, Germany) equipped with a Color View XS digital video camera. The percentage of infected cells, the number of intracellular amastigotes per infected cell and the number of amastigotes per 100 cells were evaluated by counting a total of 500 cells in 3 different experiments. The LD₅₀ was estimated as the dose that reduced the number of amastigotes per infected cell by 50%.

During the experiments described above, some trypomastigotes were released into the supernatant. These trypomastigotes were designated as trypomastigotes differentiated in the presence of venom (TDVs). To isolate TDVs from cell debris, non-viable parasites and amastigotes, the supernatant was centrifuged at 500 g for 5 min and incubated at 37 °C for 30 min. During this period, viable TDVs in the pellet moved into the supernatant medium, which was subsequently collected and centrifuged at 3000 g

for 12 min. TDVs concentrated in the pellet were monitored based on motility and the detection of trypan blue exclusion by light microscopy as described above. Next, viable TDVs were washed twice in RPMI medium and used for a new invasion assay in the absence of Cvv venom to evaluate their infectivity. TDVs were incubated in the presence of new LLC-MK₂ cells (10:1 ratio) that had been previously cultivated as described above. Infected cells were cultivated for an additional 4–5 days in RPMI containing 2% FCS at 37 °C in a 5% CO₂ humidified atmosphere without Cvv venom. As a control, LLC-MK₂ cells were infected with trypomastigotes that had been released into the supernatant of non-treated cell cultures, using the same procedures described for TDVs. Following washing in PBS, cover-slips from both control and TDV-cell interactions were collected daily, fixed and stained as described above. The numbers of intracellular amastigotes per infected cell and per 100 cells were evaluated by performing counts for a total of 500 cells in at least 3 independent experiments.

Turbidimetric assay adapted from Marinetti

Phospholipase A₂ (PLA₂) activity was determined by adapting a turbidimetric assay described previously (Marinetti, 1965). We prepared the substrate by shaking 1 chicken egg yolk in a solution of NaCl (150 mM) to a final volume of 100 ml; the substrate was stored at 4 °C prior to the reaction. In each assay, we prepared several tubes by adding a volume (0.33 ml) of a 10% dilution of the egg suspension to a solution containing NaCl (150 mM), CaCl₂ (10 mM), taurocholic acid (0.01%) and Tris-HCl (5.0 mM, pH 7.4), until a spectrophotometric absorbance between 0.62 and 0.65 at 925 nm was achieved. The tubes were kept at 37 °C under mild and constant agitation during the procedure. The reactions were started by the addition of the Cvv venom at concentrations of 0.05–10 $\mu\text{g}/\text{ml}$. The specificity of the procedure was controlled by the measurement of *para*-bromophenacyl-bromide (*p*-BPB; Sigma), a specific PLA₂ inhibitor (Ownby *et al.* 1997; Melo and Ownby, 1999), added at concentrations of 100–500 μM . Both tests were performed to evaluate the Cvv concentration range used to challenge trypomastigotes. The *p*-BPB stock solution (500 mM) was dissolved in dimethyl sulfoxide (DMSO).

Trypomastigote challenge with pBPB-inhibited Cvv venom

Trypomastigotes (CL-Brener clone) were treated for 1 day at 37 °C with 0.15, 0.3 and 0.6 $\mu\text{g}/\text{ml}$ of Cvv venom that had been previously incubated for 30 min at room temperature with 500 μM *p*-BPB, according to the protocol described by Melo and Ownby (1999).

The parasites were concomitantly treated with the same concentrations of crude venom not previously exposed to *p*-BPB. Three types of control cells were used in the absence of Cvv venom: (i) parasites incubated in RPMI medium supplemented with 10% FCS; (ii) parasites incubated with DMSO (the final concentration of DMSO in the cultures did not exceed 0.1% vol/vol and had no effect on cell lysis); and (iii) parasites incubated with *p*-BPB only. The number of living parasites was determined by counting formalin-fixed parasites in a haemocytometer chamber in at least 3 independent experiments.

Flow cytometry analysis

Epimastigotes and tissue-culture trypomastigotes at a final concentration of 1×10^6 cells/ml were treated with Cvv venom at final concentrations of 0.5–4.0 and 0.15–1.8 $\mu\text{g/ml}$ for 24 h at 28 °C and 37 °C, respectively. The viability assay was performed in a flow cytometer with propidium iodide (PI). Parasites were washed in PBS, and cells were incubated with 15 $\mu\text{g/ml}$ PI plus 10 $\mu\text{g/ml}$ rhodamine 123 (Rh123) for 15 min. Cells were kept on ice until data acquisition and analysis with a FACSCalibur Flow Cytometer (Becton-Dickinson, Franklin Lakes, NJ, USA) equipped with CellQuest software (Joseph Trotter, Scripps Research Institute, San Diego, CA, USA). A total of 10000 events were acquired in the region previously established to correspond to the parasites. Differences in the Rh123 fluorescence level between treated and control parasites were quantified using an arbitrary index of variation (IV) obtained by the equation $(MT - MC)/MC$, where MT and MC are the median fluorescence for treated and control parasites, respectively. Negative IV values correspond to depolarization of the mitochondrial membrane. Data were obtained from at least 3 independent experiments.

Scanning electron microscopy

Epimastigotes and tissue culture trypomastigotes treated with 0.5 and 0.3 $\mu\text{g/ml}$ of the Cvv crude venom for 24 h, respectively, were washed twice with PBS and fixed for 1 h with 2.5% glutaraldehyde in 0.1 M cacodylate buffer (pH 7.2) containing 5 mM calcium chloride and 2% sucrose. The parasites were then washed with the same buffer and allowed to adhere to glass cover-slips previously coated with 0.1% poly-L-lysine (MW 70 000, Sigma). After post-fixation for 15 min with 1% osmium tetroxide (OsO_4) containing 0.8% potassium ferrocyanide and 5 mM calcium chloride in 0.1 M cacodylate buffer (pH 7.2), the cells were washed, dehydrated in graded ethanol and then critical-point dried with CO_2 . The samples were allowed to adhere to scanning electron microscopy stubs coated with a 20-nm-thick gold layer in a

sputtering device and then were observed using a JEOL JSM 5310 scanning electron microscope (Tokyo, Japan) operating at 25 kV. Digital images were acquired and stored in a computer.

Transmission electron microscopy

Parasites were fixed for 1 h with 2.5% glutaraldehyde in 0.1 M cacodylate buffer (pH 7.2) containing 5 mM calcium chloride and 2% sucrose. Non-infected and infected LLC-MK₂ cells were fixed using the same fixative while still adherent, gently scraped off with a rubber policeman and were harvested by centrifugation. All samples were treated as follows: rinsed in 0.1 M cacodylate buffer (pH 7.2) containing 2% sucrose; post-fixed in 0.1 M cacodylate buffer (pH 7.2) containing 1% osmium tetroxide (OsO_4), 0.8% potassium ferrocyanide and 5 mM calcium chloride for 1 h at room temperature; dehydrated in graded acetone and then embedded in PolyBed 812 (Polysciences Inc., Warrington, PA, USA). Ultrathin sections obtained with a Leica (Nussloch, Germany) ultramicrotome were stained with uranyl acetate and lead citrate and observed using a FEI Morgagni F 268 (Eindhoven, The Netherlands) transmission electron microscope operating at 80 kV.

RESULTS

Epimastigotes were grown for 5 days in LIT medium containing different concentrations of Cvv venom, and the percentage of surviving parasites was evaluated (Table 1). The LD₅₀ (50% growth inhibition) after treatment for 24 h was 0.5 $\mu\text{g/ml}$, and after treatment for 4 and 5 days, the LD₅₀ values were 0.9 and 1 $\mu\text{g/ml}$, respectively. No growth was detected when the parasites were treated with 8–500 $\mu\text{g/ml}$ of Cvv venom. Because trypomastigote forms did not multiply and could not be maintained for several days in culture medium at 37 °C, the effect of the venom on trypomastigotes was evaluated by its capacity to cause lysis after a 24-h treatment. The LD₅₀ of Cvv venom for trypomastigotes was 0.3 $\mu\text{g/ml}$ (Table 1). The effect of Cvv venom on amastigotes is also presented in Table 1. The LD₅₀ for intracellular parasites was determined on different post-infection days, taking into account the number of amastigotes per infected cell. The LD₅₀ for intracellular amastigotes after treatment for 24 h was 0.075 $\mu\text{g/ml}$, which is the smallest value obtained among the 3 developmental forms analysed.

The loss of viability of treated epimastigotes and trypomastigotes from the supernatant was assessed by light microscopy and flow cytometry using trypan blue (data not shown) and PI labelling, respectively. Epimastigotes and trypomastigotes incubated for 24 h in the presence of 0.5 and 0.3 $\mu\text{g/ml}$ Cvv venom and then in the presence of PI presented

Table 1. Effective LD₅₀ of crude Cvv venom against epimastigote, trypomastigote and intracellular amastigote forms of *Trypanosoma cruzi*

Day of treatment	Epimastigotes	Trypomastigotes	Intracellular amastigotes ^d
1	0.5 ± 0.18 ^a	0.3 ± 0.19 ^b	0.075 ± 0.01
2	0.6 ± 0.12	Nd ^c	0.037 ± 0.03
3	0.7 ± 0.12	Nd	0.29 ± 0.03
4	0.9 ± 0.43	Nd	0.17 ± 0.02
5	1.0 ± 0.49	Nd	Nd

^a Values of LD₅₀ are expressed in µg/ml.

^b Mean ± standard deviation. All assays were performed in triplicate and in at least 3 independent experiments.

^c Not done.

^d Determined by the daily evaluation of the number of intracellular amastigotes per infected cells.

Table 2. Flow cytometry analysis of Cvv-treated *Trypanosoma cruzi* labelled with PI and Rh123

(Cvv treatment was for 1 day in LIT at 28 °C for epimastigotes and in RPMI at 37 °C for trypomastigotes.)

	µg/ml	Median Rh123	IV ^a	PI (%) ^b
Epimastigotes	0	280.0 ^c ± 14.2	0.00	0.03 ± 0.01
	0.5	67.3 ± 2.1	-0.76	59.0 ± 0.2
	1.0	64.6 ± 0.9	-0.77	67.2 ± 1.4
	2.0	48.6 ± 1.2	-0.82	89.1 ± 3.3
	4.0	45.3 ± 1.4	-0.84	99.0 ± 0.5
Trypomastigotes	0	50.2 ± 3.8	0.00	1.2 ± 0.24
	0.15	35.1 ± 0.2	-0.30	19.0 ± 3.6
	0.3	32.9 ± 0.7	-0.34	43.2 ± 0.7
	0.9	24.5 ± 0.9	-0.51	68.7 ± 2.5
	1.8	17.6 ± 1.1	-0.65	86.9 ± 3.9

^a Arbitrary Index of Variation – IV = (MT – MC)/MC, where MT and MC correspond to the median fluorescence average for treated and control parasites, respectively.

^b Percentage of PI-positive cells.

^c Data represent the mean ± standard deviation of at least 3 independent experiments.

approximately 60% and 43% non-viable cells, respectively. The values for PI labelling relative to the different venom concentrations used are shown in Table 2.

To determine whether the action of Cvv against *T. cruzi* parasites was due to the presence of enzymatic activities or to the presence of other types of molecules (e.g., alkaloids and other organic compounds, for example), we boiled the venom for different times and treated the epimastigote forms with 0.5 µg/ml of the treated venom (Fig. 1). Boiling the Cvv venom for 7.5 min did not abolish its activity completely, and a partial inhibitory effect of about 10–14% on epimastigote growth was observed up to 3 days post-treatment. Cvv venom activity was completely abolished after 15 and 30 min of boiling.

Morphological alterations in epimastigotes (Fig. 2) and trypomastigotes (Fig. 3) were observed by SEM after 1 day of treatment with 0.5 and 0.3 µg/ml of Cvv venom, respectively. Most of the treated parasites presented swelling of the body when compared to control cells (Figs 2B–D and 3B–D) and, occasionally, a complete alteration of the parasite shape was observed (Figs 2C and 3C, D). Some epimastigotes also presented an intense twisting of the cell body

(Fig. 2D). Trypomastigotes presented plasma membrane blebbing and membrane disruption with cytoplasmic eruption, indicating severe membrane disorganization (Fig. 3E).

Ultrastructural alterations caused by Cvv venom were also analysed using TEM (Figs 2 and 3). The most frequent cell alterations observed in epimastigotes were swelling of the cell body with apparent loss of normal organelle organization, vacuolization of the cytoplasm (Fig. 2E, H), swelling of the mitochondria with alterations in the mitochondrial membranes and the presence of myelin figures (Fig. 2E, F, H), and loss of cytoplasmic components (Fig. 2E, H). Eventually, several lysed epimastigotes were observed. The nuclear morphology also demonstrated alterations characterized by changes in the shape and organization of chromatin and the leakage of nuclear contents (Fig. 2G). Venom-treated trypomastigotes exhibited an enlarged space between the nucleus and the cytoplasm (Fig. 3F, inset). In trypomastigotes in which mitochondrial alterations were observed, we noted that the alterations were similar to those described for epimastigotes (Fig. 3J). The venom also caused an intense vacuolization of the cytoplasm, in which no clear structures and organelles could be

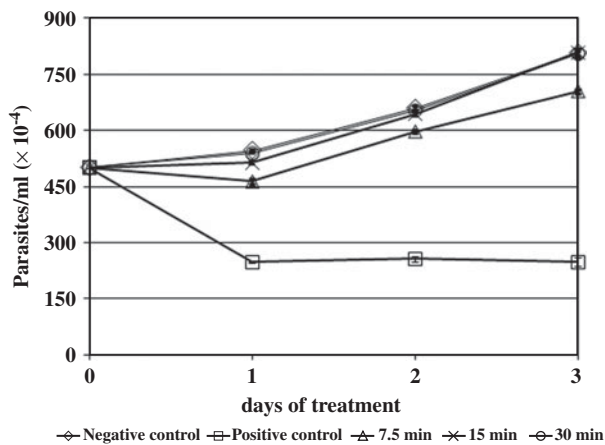


Fig. 1. Effect of boiled CvV venom on the proliferation of epimastigotes of *Trypanosoma cruzi*. Epimastigotes were incubated for up to 3 days at 28 °C with 0.5 µg/ml CvV venom previously boiled for 7.5 (-▲-), 15 (-X-) and 30 (-○-) min at 95 °C. Treatment with CvV venom previously boiled for 7.5 min caused a discrete decrease in the growth rate of the parasite, whereas no effects were observed when epimastigotes were incubated with venom that had been boiled for 15 and 30 min. All treatments were compared to treatment with LIT medium alone (-◇-) or treatment with 0.5 µg/ml CvV crude venom (-□-). Values are the means from 3 independent experiments.

observed (Fig. 3H). In most trypomastigote forms, however, we observed a dense cytoplasm with swollen organelles and blebs budding from the cell body and flagellar membranes. In some blebs, rupture of the membrane structure could be observed (Fig. 3F, G, I, J). Despite the mitochondrial damage in both epimastigotes and trypomastigotes, the integrity of the kinetoplast DNA network was apparently preserved (Figs 2F, H and 3G, I).

The observed swelling of the mitochondria prompted us to treat *T. cruzi* epimastigotes and trypomastigotes with CvV venom for 1 day, followed by labelling with Rh123 and analysis by flow cytometry. The analysis confirmed the results obtained by TEM. When epimastigotes and trypomastigotes were treated with 0.5 and 0.3 µg/ml CvV venom for 1 day, respectively, and then incubated with Rh123, a decrease in fluorescence was observed, suggesting a venom-mediated interference in the proton electrochemical potential gradient of the mitochondrial membrane. The reductions of the median fluorescence values of treated epimastigotes and trypomastigotes were dose-dependent, with IV values reaching -0.76 and -0.34 after CvV treatment at the LD₅₀, respectively (Table 2).

The marked morphological alterations in the plasma and organelle membranes led us to consider that these cellular components could be among the initial targets, or could possibly be the main targets, of the CvV venom. To evaluate PLA₂ activity in the crude venom, we performed a turbidimetric assay adapted from Marinetti (1965). Significant PLA₂

activity was observed in the crude CvV venom at the different concentrations used in this study. The absorbance of the specific substrate was reduced by almost half after the addition of 0.1–10 µg/ml CvV (Fig. 4A). The catalytic activity of PLA₂ present in 0.3 µg/ml of venom was inhibited by up to 60% in the presence of 500 µM *p*-BPB (Fig. 4B). *p*-BPB also inhibited the lytic activity of the venom in trypomastigotes. Trypomastigotes incubated for 24 h in the presence of 0.15, 0.3 and 0.6 µg/ml of CvV venom presented 30, 52 and 80% lysis rates, respectively. When trypomastigotes were similarly incubated in venom that had been previously inhibited with 500 µM *p*-BPB, the lysis rates ranged between 12 and 57% (Fig. 4C). Thus, the PLA₂ activity present in the crude venom, as determined by *p*-BPB inhibition, might be involved not only in parasite lysis but also in the other effects observed by electron microscopy.

An important aspect of chemotherapy for intracellular parasites is that the drug may also gain access to the cytoplasm of host cells, interfering with the growth or differentiation of intracellular forms. It is also possible, however, that the drug could directly affect the host, interfering with the determination of such results. Therefore, we analysed the effects of different concentrations of CvV venom on the ultrastructure and viability of non-infected LLC-MK₂ cells. Lysis, inhibition of growth and ultrastructural changes were only observed when cells were incubated with venom concentrations greater than 1 mg/ml for 24 h (data not shown). These concentrations are much higher than the LD₅₀ observed for all 3 developmental forms of the parasite (Table 1).

The observation of Giemsa-stained infected LLC-MK₂ cells before treatment by light microscopy revealed an increasing number of intracellular amastigotes on different days of the experiment (Table 3 and Fig. 5C). Infected LLC-MK₂ cells treated with different doses of CvV venom demonstrated a significant decrease in the number of parasites per infected cell (Fig. 5A) and in the number of parasites per 100 cells (Fig. 5B), as compared to the parasite numbers determined in the control cells. Infected cells incubated for 72 h in the presence of 37.5 ng/ml CvV venom presented reductions of approximately 76 and 94% in the number of parasites per infected cell and the number of parasites per 100 cells, respectively (Fig. 5C, D). The incubation of infected cells with 150 ng/ml CvV venom not only significantly inhibited the growth of intracellular forms after 72 h of treatment but also caused a slight decrease in the number of parasites per infected cell (Fig. 5A). Ultrastructural analysis of intracellular amastigotes after 48 h of treatment revealed significant changes in cell structure when compared with the control. Cells presented swollen vacuoles and lysis of the cell membrane (Fig. 5E, F). A large number of parasites were observed in the supernatant of treated cell

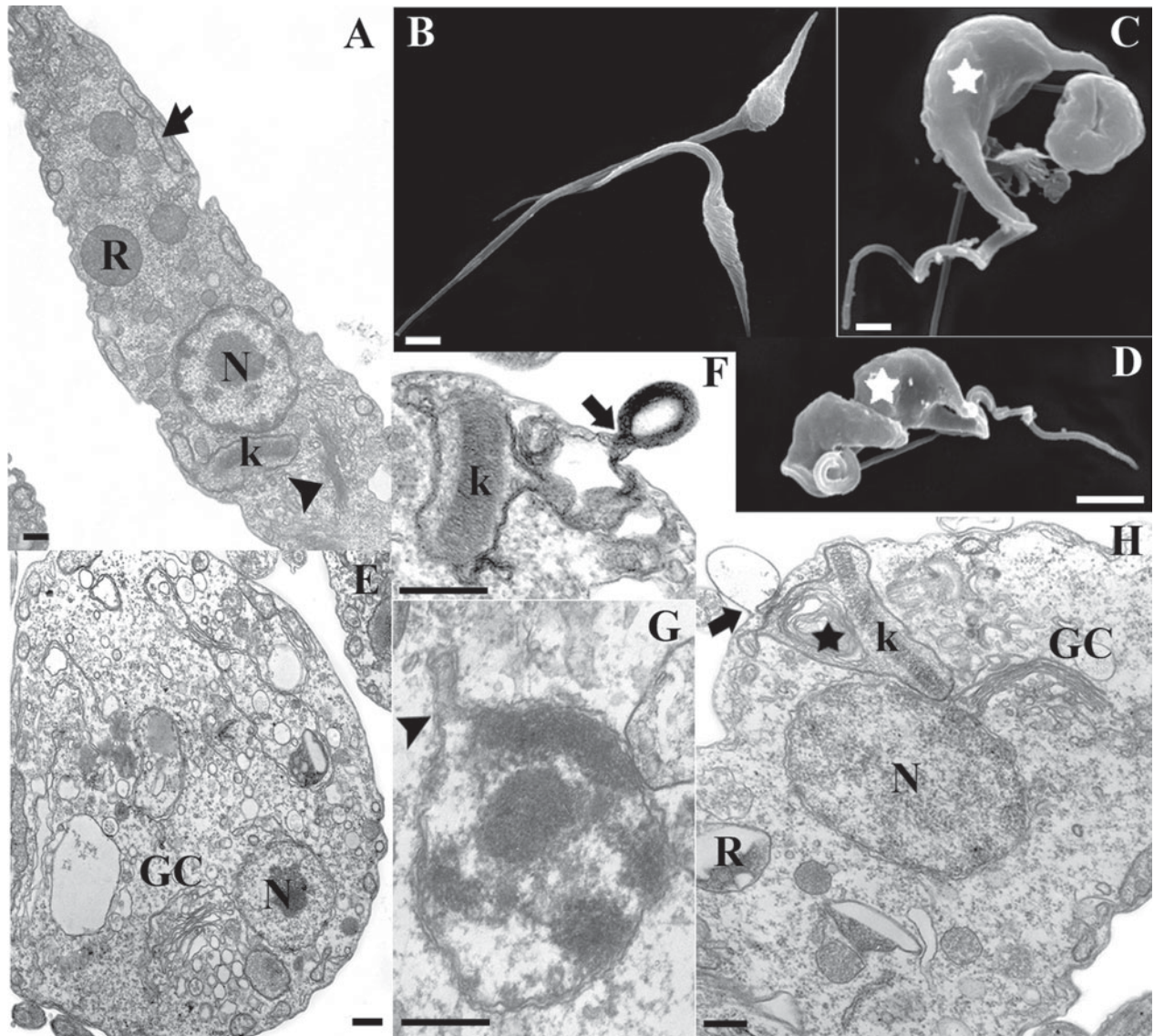


Fig. 2. Effect of Cvv venom on the ultrastructure of *Trypanosoma cruzi* epimastigotes observed using transmission (A, E–H) and scanning (B–D) electron microscopy. Parasites were treated with 0.5 µg/ml Cvv venom for 1 day. A–B: Untreated epimastigotes, showing typical elongated cell bodies and normal nuclear morphology (N), Golgi complex (arrowhead in A), kinetoplast (k), mitochondria (arrow in A) and reservosomes (R); C–D: treated parasites presenting swollen and twisted cell bodies (white star); E–H: treated parasites showing internal disorganization. The venom caused an intense swelling of the entire parasite, including all organelles, with loss of cytoplasm components (E). Blebs budding from the cell body membrane were observed (arrow in F and H). The nuclear membrane also presented morphological alterations (arrowhead in G). (H) Note the presence of myelin figures in the mitochondria (black star) and some altered reservosomes. Scale bars: A, E–G = 300 nm; B–D = 2 µm.

cultures after 48 h of treatment (Fig. 5D). The detected developmental forms were amastigotes, intermediary forms and TDV trypomastigotes, which were observed only in cells treated with Cvv venom at concentrations lower than 250 ng/ml.

Trypan blue staining of TDVs revealed that 89% of the parasites were non-viable, and the ultrastructural analysis showed intense swelling of different organelles and remarkable internal disorganization (Fig. 6B), including alterations of the mitochondria (Fig. 6B, C) and leakage of nuclear content (Fig. 6C). Taking into account the possibility that even 10% viability could provide sufficient parasites to

perpetuate the infection, we decided to use those TDVs for a new infection challenge in the absence of Cvv venom (Fig. 6). The isolation of viable TDVs and control trypomastigotes is based on a mild centrifugation of the cell culture medium followed by incubation at 37 °C, at which time viable and mobile trypomastigote forms leave the pellet and are present in the supernatant, from which they can be harvested by an additional centrifugation. We observed a progressive reduction of approximately 63–92% of the number of infected cells from 48 to 144 h post-infection when LLC-MK₂ cells were infected with TDVs (Table 3). The number of

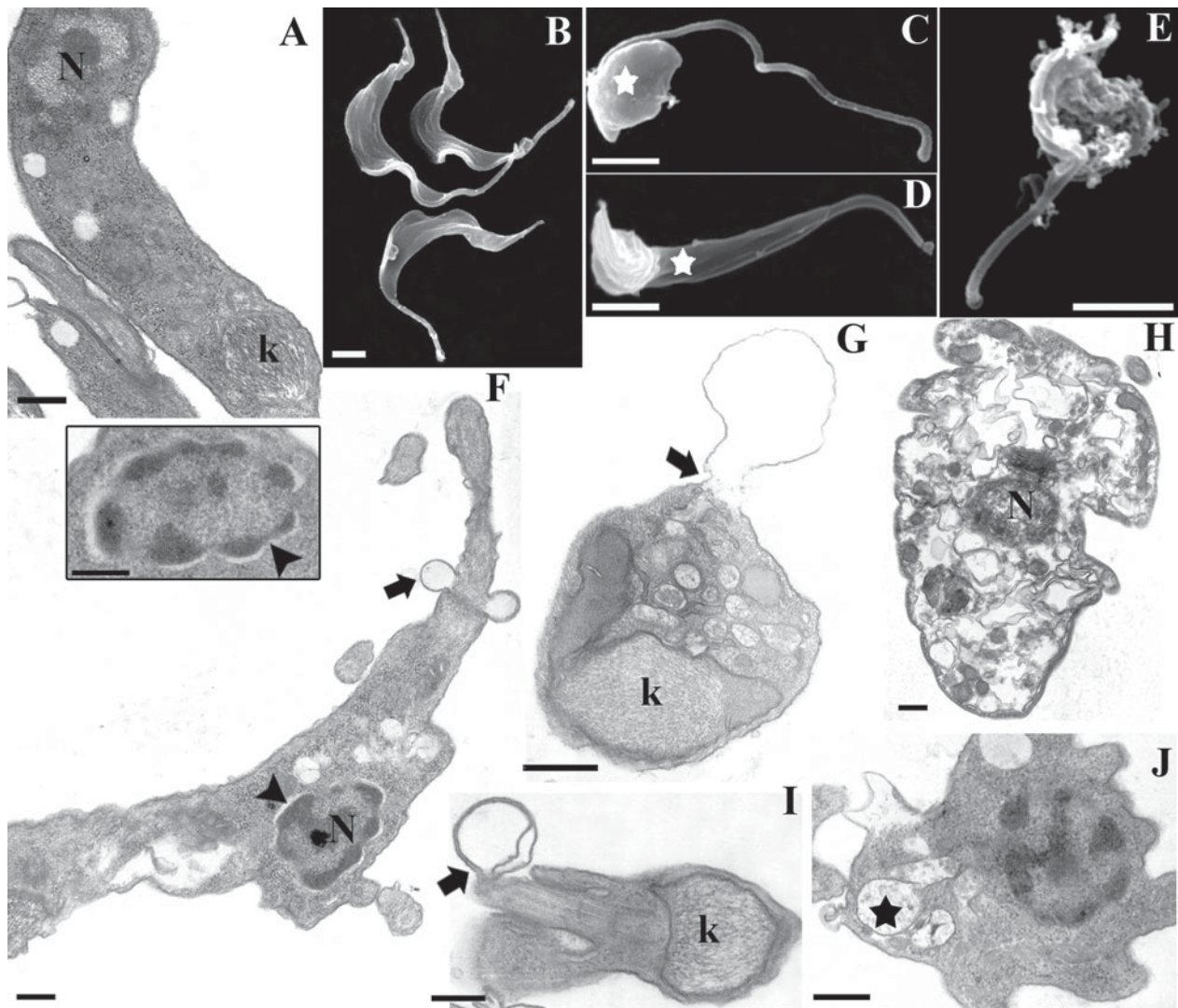


Fig. 3. Effect of CvV venom on the ultrastructure of *Trypanosoma cruzi* trypomastigotes observed using transmission (A, F–J) and scanning (B–E) electron microscopy. Parasites were treated with $0.3 \mu\text{g/ml}$ CvV venom for 1 day. (A, B) Control parasites presenting a typical morphology with normal characteristics of the nucleus (N) and kinetoplasts (k). (C–E) Treated parasites presenting swollen and twisted cell bodies (white star in C and D), loss of membrane integrity and cell lysis (E and H). The main changes in the ultrastructure of the trypomastigotes observed by TEM were shrinkage of the nuclear membrane (arrowhead in the inset and in F), the presence of clear areas in the cytoplasm (star in F), blebs budding from the cell body (arrow in G) and from the flagellar membrane (arrows in F and I), and the presence of swollen organelles (G). (J) Note the swollen mitochondria (black star). Scale bars: A, F–J = 300 nm; B–E = $2 \mu\text{m}$.

amastigotes per 100 cells was also significantly reduced during the same period. After 48 h of infection, 15 parasites derived from TDVs were observed per 100 host cells, representing a reduction of about 74% with respect to the number of parasites observed in cells infected with control trypomastigotes. After 144 h of infection, a reduction of approximately 96% was observed (Table 3).

DISCUSSION

The development of anti-parasite chemotherapy could emerge from the screening of natural products such as animal venoms and plant essential oils. Snake venoms are complex mixtures of a large

number of biologically active polypeptides, apparently inactive polypeptides of unknown significance, and small molecules such as adrenaline (Harris and Cullen, 1990; Passero *et al.* 2007).

Epimastigotes (the insect-borne stage) and trypomastigotes (the infective flagellate form) of *T. cruzi* were found to be sensitive to the venom. In comparison with previous studies using distinct crude venoms against epimastigote forms of *T. cruzi*, we observed that the $\text{LD}_{50}/\text{day}$ of CvV for epimastigotes ($0.5 \mu\text{g/ml}$) was between those obtained with the crude venom of *B. jararaca* and *C. cerastes* (Fernandez-Gomez *et al.* 1994; Gonçalves *et al.* 2002; Deolindo *et al.* 2005). The lysis of trypomastigote forms, as performed in this study, was not

Table 3. Evolution of intracellular development of TDV parasites in different post-infection periods

Time after infection (h)	Control% of infected cells	TDV% of infected cells	% Reduction	Control no. of amast./100 cells	TDV no. of amast./100 cells	% Reduction
48	27.5 ± 3.2*	9.7 ± 0.5	63.0 ± 2.0	58.4 ± 20.1	15.2 ± 2.5	74.0 ± 4.3
72	29.4 ± 4.8	9.7 ± 0.8	67.1 ± 2.9	71.8 ± 25.1	14.5 ± 2.3	79.7 ± 3.2
96	32.8 ± 9.4	4.4 ± 1.7	86.5 ± 5.3	84.2 ± 32.3	6.4 ± 2.0	92.4 ± 2.3
120	42.4 ± 15.8	3.7 ± 0.4	91.2 ± 1.1	106.8 ± 39.4	5.9 ± 0.2	94.4 ± 0.2
144	43.9 ± 17.0	3.5 ± 0.3	92.0 ± 0.7	114.7 ± 38.5	4.4 ± 0.6	96.1 ± 0.5

* Mean ± standard deviation. All assays were performed in triplicate and in at least 3 independent experiments.

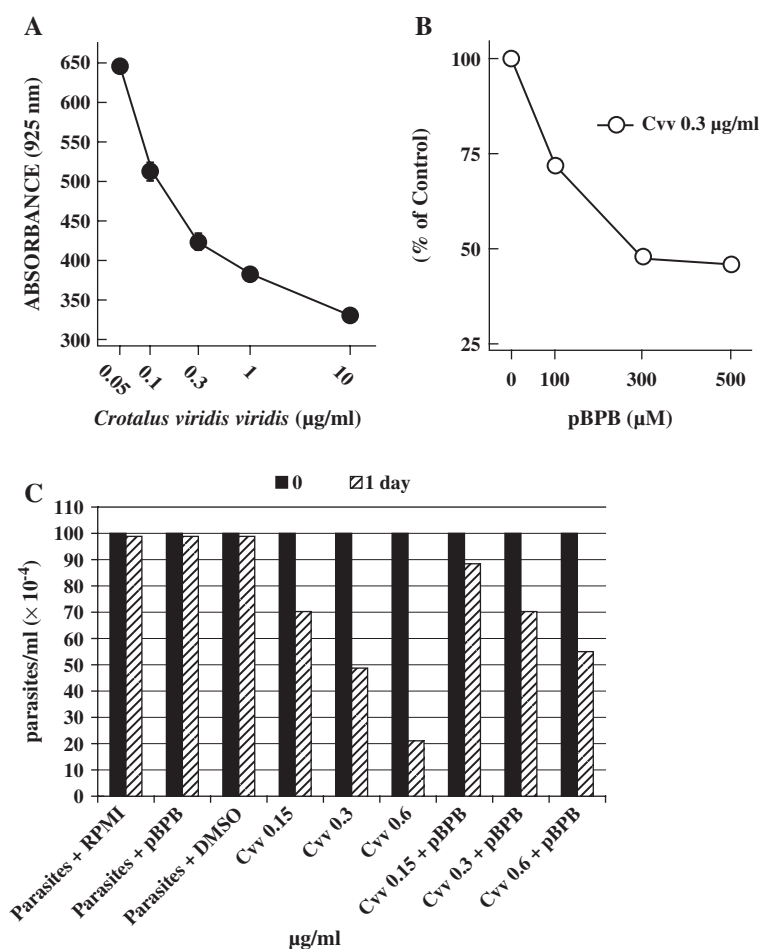


Fig. 4. PLA₂ activity of CvV crude venom and inhibition by *p*-BPB. (A) Curve showing the phospholipase activity of CvV venom (0.05–10 µg/ml) in the presence of specific substrate. The enzyme activity was measured 30 min after addition of CvV venom (0.05–10 µg/ml) to the substrate solution. (B) Effect of *p*-BPB (100–500 µM) on the phospholipase activity of CvV venom (0.3 µg/ml). Data are expressed as means ± S.E.M. ($n = 5$). (C) Inhibition of the PLA₂ activity of CvV venom treated with *p*-BPB. Lysis of trypomastigotes in the presence of CvV venom plus *p*-BPB was evaluated. Trypomastigotes were incubated for 1 day in RPMI medium in the presence of 0.15, 0.3 and 0.6 µg/ml of normal or *p*-BPB (500 µM)-treated CvV venom. The following controls were used: (i) parasites incubated in RPMI medium supplemented with 10% FCS (parasites + RPMI); (ii) parasites incubated in RPMI medium containing DMSO at the same dilution present in the *p*-BPB final solutions (parasites + DMSO); (iii) parasites incubated in RPMI medium containing 500 µM *p*-BPB (parasites + *p*-BPB).

evaluated in other studies of snake venoms. Although the LD₅₀ value for trypomastigotes (0.3 µg/ml) was lower than that obtained for epimastigotes, the statistical analysis revealed no differences between the LD₅₀ values for both developmental forms. Flow cytometry and ultrastructural analysis, however,

indicated that CvV venom possesses different mechanisms of action against epimastigotes and trypomastigotes, as will be discussed later.

Labelling with PI and Rh123 indicated different behaviours for epimastigotes and trypomastigotes in the presence of CvV venom. After incubation of both

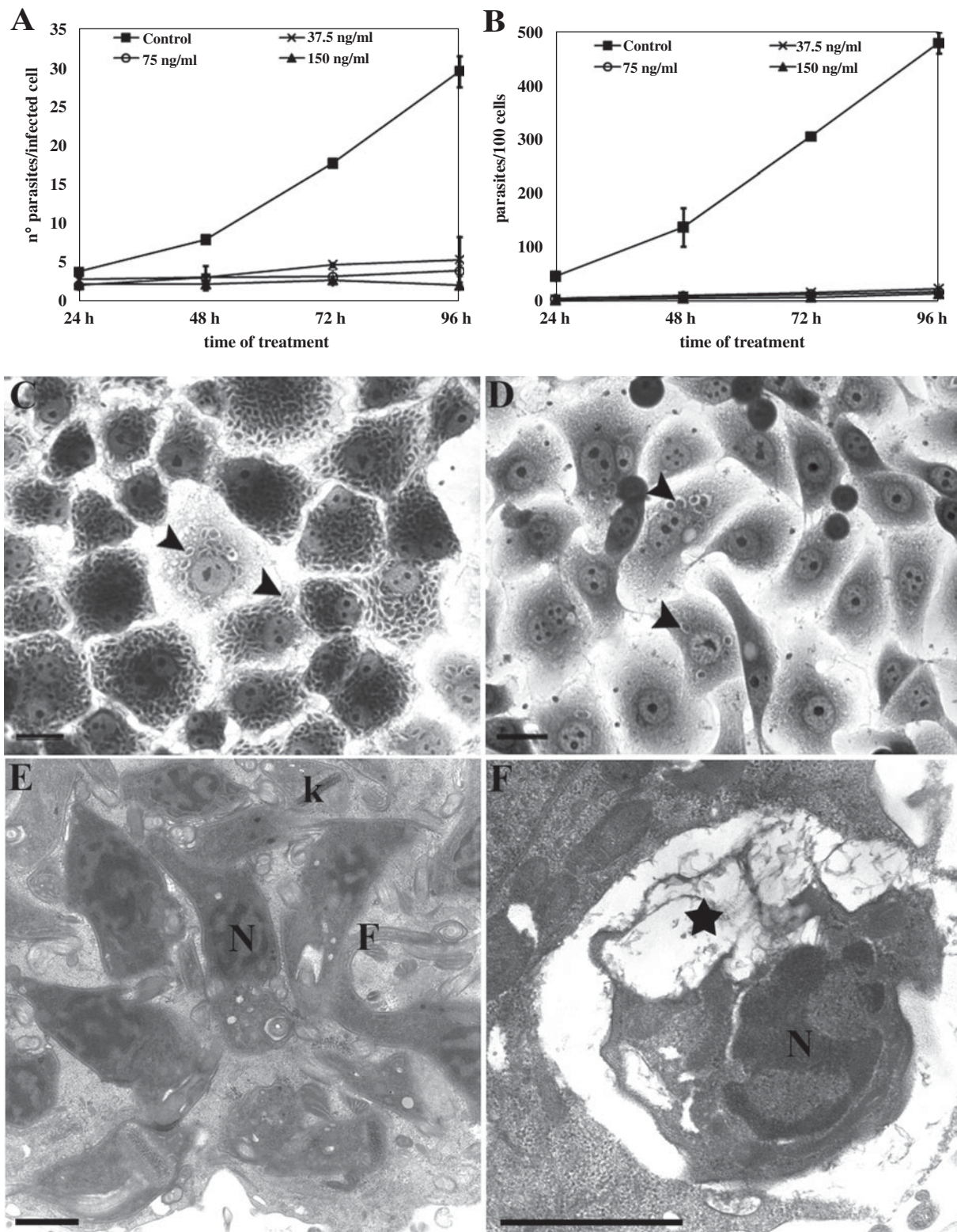


Fig. 5. Light (C–D) and transmission electron microscopy (E–F) of *Trypanosoma cruzi*-infected LLC-MK₂ cells following Cvv venom treatment. (A–B) Infection of LLC-MK₂ cells is almost abolished after treatment with 150 ng/ml Cvv venom for 4 days. The low infection level was maintained by incubation with 37.5 to 75 ng/ml Cvv venom during the same treatment period. (C, E) Control cells after 72 h of infection showing high infection rates with many intracellular amastigotes (arrowheads). By TEM, the intracellular parasites presented a typical morphology of the nucleus (N), kinetoplast (k), and flagellum (F). (D) Cells treated with 37.5 ng/ml for 48 h showed a very low level of infection with few intracellular amastigotes (arrowheads). The LLC-MK₂ cells demonstrated normal 4-day culture without alterations in size or shape. (F) Intracellular amastigotes after 48 h of treatment with 37.5 ng/ml Cvv venom presented an intense swelling of the cytoplasmic compartments (black star) with rupture of the cell membrane. Scale bars: C–D = 20 μ m; E–F = 1 μ m.

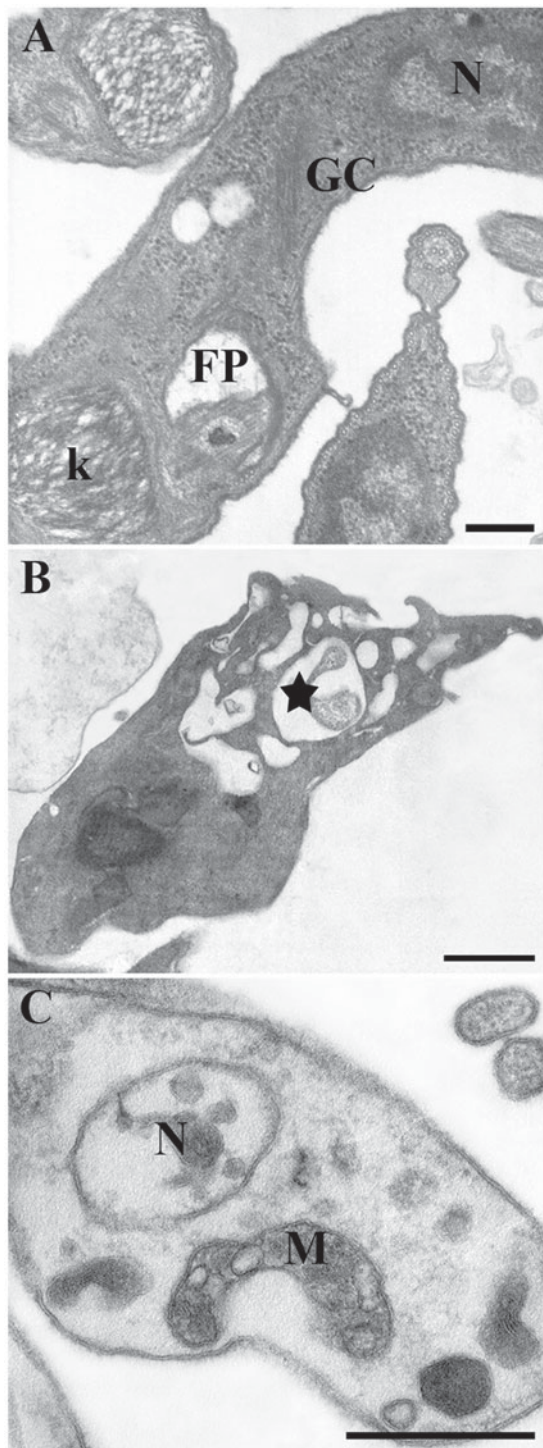


Fig. 6. Ultrastructural appearance and behaviour of TDVs. Transmission electron microscopy analysis of TDVs obtained from the supernatant of Cvv venom-treated LLC-MK₂ cells (B–C) showing profound internal disorganization with many swollen organelles (star in B); changes in the organization of the chromatin and leakage of the nuclear content like that of the cytoplasm (C); mitochondrial swelling and loss of matrix content, as compared to control trypomastigotes (A). Nucleus (N), mitochondria (M) Golgi complex (GC), kinetoplast (k) and flagellar pocket (FP). Scale bars = 0.3 μ m.

forms with their respective Cvv LD₅₀, 60% and 40% of the epimastigotes and trypomastigotes, respectively, were PI-positive, indicating that lysis of the cell membrane is an important aspect of the effect of the venom. The analysis of Rh123 showed that at the LD₅₀, reductions of approximately 76% and 34% of the numbers of labelled cells were observed for epimastigotes and trypomastigotes, respectively.

Ultrastructural analysis of treated epimastigotes and trypomastigotes revealed differences in the effects of Cvv venom that corroborate the flow cytometry results obtained for PI and Rh123 staining. Although similar morphological changes could be observed in both developmental forms, epimastigotes were significantly more swollen and presented greater mitochondrial damage with myelin figures than trypomastigotes. Most of the trypomastigotes had a dense cytoplasm and non-swollen mitochondria, as shown in Fig. 3G. The most characteristic lesion observed in trypomastigotes was the presence of large membrane projections budding from the cell body and the flagellum, confirming the action of the venom on the parasite membrane.

All of the observed morphological changes in addition to the flow cytometry data suggest that Cvv venom causes necrotic cell death in *T. cruzi*. Our results are similar to those of other groups who have characterized the activities of several drugs against *T. cruzi* epimastigote and trypomastigote forms (Menna-Barreto *et al.* 2009). However, more studies are necessary to characterize this phenotype.

The most important finding of the present study was the effect of Cvv venom on the intracellular cycle of the parasite. The proliferation of amastigotes, the intracellular stage of the protozoan responsible for the maintenance of infection in chagasic patients, was inhibited at concentrations of venom significantly lower than those necessary to kill trypomastigotes, or even to cause damage to the host cells. The Cvv venom was at least 10 000-fold more toxic to the amastigotes than to LLC-MK₂ cells. In addition, at venom concentrations that still allowed the propagation of the entire intracellular cycle, we observed after 3–4 days of infection the presence of intermediary and trypomastigote forms in the cell culture medium that presented several structural changes similar to those described for the other venom-treated parasites. We termed these parasites TDVs and found that they were unable to initiate a new intracellular cycle even in the absence of venom. This finding was confirmed by not only the reduced number of infected cells in culture but also the number of amastigotes per 100 cells.

We did not elucidate the exact mechanism responsible for the trypanocidal action of Cvv venom, but in contrast to *B. jararaca* venom, the activity of Cvv venom was inhibited after boiling for 30 min (Gonçalves *et al.* 2002), suggesting the involvement of peptides and enzymes in the process.

Some PLA₂s isolated from snake venoms have been reported to possess the ability to induce toxicity in muscle cells, with remarkable effects on the plasma membrane and mitochondria (Gutiérrez and Ownby, 2003). Ownby *et al.* (1997) have shown that Cvv venom contains a basic polypeptide similar to the PLA₂ myotoxins present in other snake venoms that have been shown to cause lysis of the plasma membrane. The general consensus on the mechanism of action of PLA₂s is that the plasma membrane is the primary site of action. Our results demonstrating the partial inhibition of Cvv crude venom activity in the presence of *p*-BPB indicated that among the molecules present in the crude extract cells, PLA₂ might act directly on the parasite, and other compounds present in the Cvv total extract could function synergistically with PLA₂ on the parasites. This could explain the remaining action (about 30%) of the venom partially inhibited with *p*-BPB under conditions of 0.3 µg/ml Cvv venom and LD₅₀/1 day treatment.

In addition to different enzymatic activities, some previous studies have shown that L-amino acid oxidases (L-AAOs) isolated from different snake venoms have the ability to kill *Leishmania* spp. and *T. cruzi* trypomastigotes (Tempone *et al.* 2001; Ciscotto *et al.* 2009). The enzymes that are largely responsible for the yellow colour of snake venoms convert free amino acids into α -keto acids and produce hydrogen peroxide and ammonia (Tu, 1996). Cvv venom exhibits an intense yellow colour, suggesting the presence of L-AAO activity. A synergistic action between PLA₂ and L-AAO could be responsible to the observed effects on the parasites.

It is well known that the major limitation of the drugs currently available for Chagas' disease is the reduction of anti-amastigote activity during the chronic form of the disease, probably due to the limited tissue penetration (Urbina and Docampo, 2003). The present study demonstrates the potential effects of Cvv venom mainly against the intracellular forms of the parasite. The search for alternative treatments with different drugs or different drug combinations may improve the efficacy of treatment for Chagas disease.

ACKNOWLEDGMENTS

We thank Mr Antonio Bosco Carlos, Ms Edna Lúcia dos Santos Rocha and Ms Lusinete da Rocha Bonfim for valuable technical assistance.

FINANCIAL SUPPORT

The present work was supported by grants from Conselho Nacional de Desenvolvimento Científico e Tecnológico (CNPq-302440/2008-9) and Fundação Carlos Chagas Filho de Amparo a Pesquisa do Estado do Rio de Janeiro (FAPERJ-E-26/102.299/2009 and Pensa Rio -E-26/110.401/2007).

REFERENCES

- Araya, C. and Lomonte, B.** (2007). Antitumor effects of cationic synthetic peptides derived from Lys49 phospholipase A2 homologues of snake venoms. *Cell Biology International* **31**, 263–268. doi: 10.1016/j.cellbi.2006.11.007.
- Bisaggio, D. F., Adade, C. M. and Souto-Pradón, T.** (2008). In vitro effects of suramin on *Trypanosoma cruzi*. *International Journal of Antimicrobial Agents* **31**, 282–286. doi: 10.1016/j.ijantimicag.2007.11.001.
- Bisaggio, D. F. R., Campanati, L., Pinto, R. C. V. and Souto-Pradón, T.** (2006). Effect of suramin on trypomastigote forms of *Trypanosoma cruzi*: Changes on cell motility and on the ultrastructure of the flagellum-cell body attachment region. *Acta Tropica* **98**, 162–175. doi: 10.1016/j.actatropica.2006.04.003.
- Camargo, E. P.** (1964). Growth and differentiation in *Trypanosoma cruzi*. I. Origin of metacyclic trypanosomes in liquid media. *Revista do Instituto de Medicina Tropical de São Paulo* **6**, 93–100.
- Ciscotto, P., Machado de Avila, R. A., Coelho, E. A. F., Oliveira, J., Diniz, C. G., Farias, L. M., Carvalho, M. A. R., Maria, W. S., Sanchez, E. F., Borges, A. and Chávez-Olórtegui, C.** (2009). Antigenic, microbicidal and antiparasitic properties of an L -amino acid oxidase isolated from *Bothrops jararaca* snake venom. *Toxicon* **53**, 330–341. doi: 10.1016/j.toxicon.2008.12.004.
- Corrêa, M. C. C. Jr., Maria, D. A., Moura-da-Silva, A. M., Pizzocaro, K. F. and Ruiz, I. R. G.** (2002). Inhibition of melanoma cells tumorigenicity by the snake venom toxin jararhagin. *Toxicon* **40**, 739–748. doi: 10.1016/S0041-0101(01)00275-6.
- Coura, J. R. and De Castro, S. L.** (2002). A critical review on Chagas' disease chemotherapy. *Memórias do Instituto Oswaldo Cruz* **97**, 3–24. doi: 10.1590/S0074-02762002000100001.
- Deolindo, P., Teixeira-Ferreira, A. S., Melo, E. J. T., Arnholdt, A. C. V., De Souza, W., Alves, E. W. and DaMatta, R. A.** (2005). Programmed cell death in *Trypanosoma cruzi* induced by *Bothrops jararaca* venom. *Memórias do Instituto Oswaldo Cruz* **100**, 33–38. doi: 10.1590/S0074-02762005000100006.
- El-Rafael, M. F. and Sarkar, N. H.** (2009). Snake venom inhibits the growth of mouse mammary tumor cells *in vitro* and *in vivo*. *Toxicon* **54**, 33–41. doi: 10.1016/j.toxicon.2009.03.017.
- Fernandez-Gomez, R., Zerrouk, H., Sebti, F., Loyens, M., Benslimane, A. and Ouaisi, M. A.** (1994). Growth inhibition of *Trypanosoma cruzi* and *Leishmania donovani infantum* by different snake venoms: Preliminary identification of proteins from *Cerastes cerastes* venom which interacts with the parasites. *Toxicon* **32**, 875–882. doi: 10.1016/0041-0101(94)90366-2.
- Fernandez, J. H., Neshich, G. and Camargo, A. C.** (2004). Using bradykinin-potentiating peptide structures to develop new antihypertensive drugs. *Genetics and Molecular Research* **3**, 554–563.
- Gonçalves, A. R., Soares, M. J., De Souza, W., DaMatta, R. A. and Alves, E. W.** (2002). Ultrastructural alterations and growth inhibition of *Trypanosoma cruzi* and *Leishmania major* induced

- by *Bothrops jararaca* venom. *Parasitology Research* **88**, 598–602. doi: 10.1007/s00436-002-0626-3.
- Gutiérrez, J. M. and Ownby, C. L.** (2003). Skeletal muscle degeneration induced by venom phospholipases A₂: insights into the mechanisms of local and systemic myotoxicity. *Toxicon* **42**, 915–931. doi: 10.1016/j.toxicon.2003.11.005.
- Harris, J. B. and Cullen, M. J.** (1990). Muscle necrosis caused by snake venoms and toxins. *Electron Microscopy Reviews* **3**, 183–211.
- Koh, D. C. I., Armugam, A. and Jeyaseelan, K.** (2006). Snake venom components and their applications in biomedicine. *Cellular and Molecular Life Sciences* **63**, 3030–3041. doi: 10.1007/s00018-006-6315-0.
- Marinetti, G. V.** (1965). The action of phospholipase A on lipoproteins. *Biochimica et Biophysica Acta* **98**, 554–565. doi: 10.1016/0005-2760(65)90152-9.
- Melo, P. A. and Ownby, C. L.** (1999). Ability of wedelolactone, heparin, and *para*-bromophenacyl bromide to antagonize the myotoxic effects of two crotaline venoms and their PLA₂ myotoxins. *Toxicon* **37**, 199–215. doi: 10.1016/S0041-0101(98)00183-4.
- Menna-Barreto, R. F. S., Salomão, K., Dantas, A. P., Santa-Rita, R. M., Soares, M. J., Barbosa, H. S. and De Castro, S. L.** (2009). Different cell death pathways induced by drugs in *Trypanosoma cruzi*: An ultrastructural study. *Micron* **40**, 157–168. doi: 10.1016/j.micron.2008.08.003.
- Moncayo, A. and Silveira, A. C.** (2009). Current epidemiological trends for Chagas disease in Latin America and future challenges in epidemiology, surveillance and health policy. *Memórias do Instituto Oswaldo Cruz* **104**, 17–30. doi: 10.1590/S0074-02762009000900005.
- Newman, R. A., Vidal, J. C., Viskatis, L. J., Johnson, J. and Etcheverry, M. A.** (1993). VRCTC-310-1 novel compound of purified animal toxins separated anti-tumor efficacy from neurotoxicity. *Investigational New Drugs* **11**, 151–159.
- Ownby, C. L., Colberg, T. R. and White, S. P.** (1997). Isolation, characterization and crystallization of a phospholipase A₂ myotoxin from the venom of the prairie rattlesnake (*Crotalus viridis viridis*). *Toxicon* **35**, 111–124. doi: 10.1016/S0041-0101(96)00054-2.
- Pai, L. H., Wittes, R., Setser, A., Willingham, M. C. and Pastan, I.** (1996). Treatment of advanced solid tumors with immunotoxin LMB-1: on antibody linked to pseudomonas exotoxin. *Nature Medicine* **2**, 350–353.
- Papo, N. and Shai, Y.** (2003). New lytic peptides based on the D,L-amphipathic helix motif preferentially kill tumor cells compared to normal cells. *Biochemistry* **42**, 9346–9354. doi: 10.1021/bi027212o.
- Papo, N., Shahar, M., Eisenbach, L. and Shai, Y.** (2003). A novel lytic peptide composed of DL-amino acids selectively kills cancer cells in culture and in mice. *The Journal of Biological Chemistry* **278**, 21018–21023. doi: 10.1074/jbc.M211204200.
- Papo, N., Braunstein, A., Eshhar, Z. and Shai, Y.** (2004). Suppression of human prostate tumor growth in mice by a cytolytic D-, L- amino acid peptide: membrane lysis, increased necrosis, and inhibition of prostate-specific antigen secretion. *Cancer Research* **64**, 5779–5786.
- Passero, L. F. D., Tomokane, T. Y., Corbett, C. E. P., Laurenti, M. D. and Toyama, M. H.** (2007). Comparative studies of the anti-leishmanial activity of three *Crotalus durissus* ssp. venoms. *Parasitology Research* **101**, 1365–1371. doi: 10.1007/s00436-007-0653-1.
- Tempone, A. G., Andrade, H. F., Spencer, P. J., Lourenço, C. O., Rogero, J. R. and Nascimento, N.** (2001). *Bothrops moojeni* venom kills *Leishmania* spp. with hydrogen peroxide generated by its L-amino acid oxidase. *Biochemical and Biophysical Research Communications* **280**, 620–624. doi: 10.1006/bbrc.2000.4175.
- Tempone, A. G., Sartorelli, P., Mady, C. and Fernandes, F.** (2007). Natural products to anti-trypanosomal drugs: an overview of new drug prototypes for American Trypanosomiasis. *Cardiovascular & Hematological Agents in Medicinal Chemistry* **5**, 222–235.
- Toyama, M. H., Toyama, D. de O., Passero, L. F., Laurenti, M. D., Corbett, C. E., Tomokane, T. Y., Fonseca, F. V., Antunes, E., Joazeiro, P. P., Beriam, L. O., Martins, M. A., Monteiro, H. S. and Fonteles, M. C.** (2006). Isolation of a new L-amino acid oxidase from *Crotalus durissus cascavella* venom. *Toxicon* **47**, 47–57. doi: 10.1016/j.toxicon.2005.09.008.
- Tsai, I.-H., Wang, Y.-M., Chen, Y.-H. and Tu, A. T.** (2003). Geographic variations, cloning, and functional analyzes of the venom acidic phospholipases A₂ of *Crotalus viridis viridis*. *Archives of Biochemistry and Biophysics* **411**, 289–296. doi: 10.1016/S0003-9861(02)00747-6.
- Tu, A. T.** (1996). Overview of snake venom chemistry. In *Natural Toxins II* (ed. Singh, B. R. and Tu, A. T.), pp. 37–63. Plenum Press, New York, USA.
- Urbina, J. A. and Docampo, R.** (2003). Specific chemotherapy of Chagas disease: controversies and advances. *Trends in Parasitology* **19**, 495–501. doi: 10.1016/j.pt.2003.09.001.
- Zhang, Y. J., Wang, J. H., Lee, W. H., Wang, Q., Liu, H., Zheng, Y. T. and Zhang, Y.** (2003). Molecular characterization of *Trimeresurus stejnegeri* venom L-amino acid oxidase with potential anti-HIV activity. *Biochemical and Biophysical Research Communications* **309**, 598–604. doi: 10.1016/j.bbrc.2003.08.044.
- Zhou, Q., Sherwin, R. P., Parrish, C., Richters, V., Groshen, S. G., Tsao-Wei, D. and Markland, F. S.** (2000). Contortrostatin, a dimeric disintegrin from *Agkistrodon contortrix contortrix*, inhibits breast cancer progression. *Breast Cancer Research* **61**, 249–260. doi: 10.1023/A:1006457903545.
- Zieler, H., Keister, D. B., Dvorak, J. A. and Ribeiro, M. C.** (2001). A snake venom phospholipase A₂ blocks malaria parasite development in the mosquito midgut by inhibiting ookinete association with the midgut surface. *The Journal of Experimental Biology* **204**, 4157–4167.